

Late-time drainage from a sloping Boussinesq aquifer

Patrick W. Bogaart,¹ David E. Rupp,² John S. Selker,³ and Ype van der Velde¹

Received 4 March 2013; revised 9 October 2013; accepted 15 October 2013; published 20 November 2013.

[1] Numerical solutions to the nonlinear Boussinesq equation, applied to a steeply sloping aquifer and assuming uniform hydraulic conductivity, indicate that late-time recession discharge decreases nearly linearly in time. When recession discharge is characterized by $-dQ/dt = aQ^b$, this is equivalent to constant dQ/dt or $b = 0$. This result suggests that a previously reported exponential decrease with time ($b = 1$) of modeled recession discharge from a similar sloping aquifer represented by the same equation appears to be an artifact of the numerical solution scheme and its interpretation. Because the linearly decreasing recession discharge ($b = 0$) is not known from field studies, these findings challenge the application of a nonlinear Boussinesq framework assuming uniform conductivity and geometric similarity to infer hydraulic properties of sloping aquifers from observations of streamflow. This finding also questions the validity of the physical interpretation of the exponential decline in late time resulting from the commonly used linearized form of the Boussinesq equation, opposed to the full nonlinear equation, when applied under these conditions. For this reason, application of the linearized equation to infer hydraulic properties of sloping aquifers is also challenged, even if the observed recession is consistent with that of the linearized Boussinesq equation.

Citation: Bogaart, P. W., D. E. Rupp, J. S. Selker, and Y. van der Velde (2013), Late-time drainage from a sloping Boussinesq aquifer, *Water Resour. Res.*, 49, 7498–7507, doi:10.1002/2013WR013780.

1. Introduction

[2] Following the pioneering recession flow analysis work by *Brutsaert and Nieber* [1977], *Troch et al.* [1993], and *Szilagyi et al.* [1998], attempts have been made to use analytical solutions to (linearizations of) the nonlinear Boussinesq equation to infer hydraulic properties of sloping aquifers, e.g., while using the linearized Boussinesq equation [*Huyck et al.*, 2005], focusing on the rising limb of a hydrograph [*Pauwels and Troch*, 2010], or testing a hill-slope subsurface flow similarity number [*Lyon and Troch*, 2007]. These attempts make use of the method of hydrograph analysis, first introduced by *Brutsaert and Nieber* [1977], when considering recession flow from horizontal aquifers. *Brutsaert and Nieber* [1977] showed how under certain initial and boundary conditions, the recession discharge $Q(t)$ from a horizontal Boussinesq aquifer can take the form

$$-\frac{dQ}{dt} = aQ^b \quad (1)$$

where a is a function of the aquifer properties and b is a constant. For instance, for flat-lying aquifers, characterized by spatially and vertically uniform saturated hydraulic conductivity k and drainable porosity (or specific yield) f , it can be shown analytically [*Brutsaert and Nieber*, 1977] that after initial effects are dissipated (“late time”)

$$a = 4.8038 \frac{k^{1/2} L_d}{fA^{3/2}} \quad (2a)$$

$$b = 3/2 \quad (2b)$$

with A catchment area and L_d/A drainage density.

[3] The direct use of equation (2a) to infer, for instance, k from recession data and known A , L_d , and f , requires that $b = 3/2$ and that the assumptions underlying the nonlinear Boussinesq equation hold. Any $b \neq 3/2$ thus raises challenges for the use of equation (2a) to infer k for flat-lying aquifers. Indeed, in applications of equation (2a), *Brutsaert and Nieber* [1977] and *Troch et al.* [1993] showed that their discharge data suggested $b = 3/2$ during late time. *Eng and Brutsaert* [1999] and *Brutsaert and Lopez* [1998] found $b = 1$, and consequently replaced equation (2a) with a similar approach based on the linearized Boussinesq equation, that does correspond to $b = 1$. Using an alternative set of assumptions, especially a drawdown that is small relative to saturated thickness, *van de Giesen et al.* [2005] demonstrated that solutions to aquifer recession based on the Laplace equation leads to $b = 1$ during late time as well.

[4] It bears noting that the use of a similar approach to infer aquifer properties for sloping hillslopes or catchments

¹Copernicus Institute of Sustainable Development, Environmental Sciences group, Utrecht University, Utrecht, Netherlands.

²Oregon Climate Change Research Institute, College of Earth, Ocean, and Atmospheric Sciences, Oregon State University, Corvallis, Oregon, USA.

³Department of Biological and Ecological Engineering, Oregon State University, Corvallis, Oregon, USA.

Corresponding author: P. W. Bogaart, Copernicus Institute of Sustainable Development, Environmental Sciences Group, Utrecht University, PO Box 80115, NL-3508 TC Utrecht, The Netherlands. (p.w.bogaart@uu.nl)

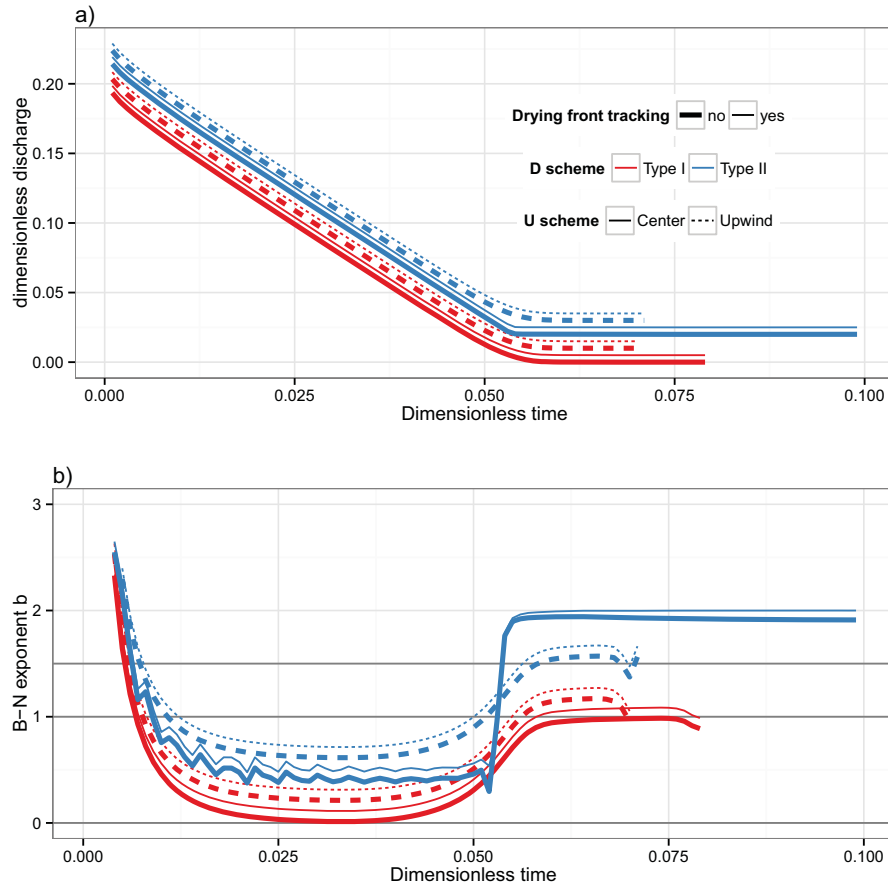


Figure 1. (a) Nondimensional hydrographs and (b) evolution of recession parameter b , for different spatial difference schemes associated with the diffusion term of the Boussinesq equation (“ D -scheme”) and the advection term (“ U -scheme”), and optional drying front tracking, using a Steady-State I.C. Note that individual curves are offset by 0.005 (discharge) or 0.1 (b) to distinguish them. Gray horizontal lines indicate $b = 0, 1, 3/2$.

hinges on the correspondence between observed values of b , and the valid value of b associated with the version of the Boussinesq equation and the underlying assumptions made.

[5] The nonlinear Boussinesq equation for a sloping aquifer with gradient α is derived by combining the Darcy equation

$$q = -kh^* \left(\frac{\partial h^*}{\partial x^*} \cos \alpha + \sin \alpha \right) \quad (3)$$

with the continuity equation

$$f \frac{\partial h^*}{\partial t^*} = - \frac{\partial}{\partial x^*} (q) + N \quad (4)$$

yielding [Brutsaert, 1994]

$$\frac{\partial h^*}{\partial t^*} = \frac{k}{f} \frac{\partial}{\partial x^*} \left[h^* \left(\frac{\partial h^*}{\partial x^*} \cos \alpha + \sin \alpha \right) \right] + \frac{N}{f} \quad (5)$$

where x^* is a coordinate along the hillslope ($x^* = 0$ at the foot), $h^* = h(x^*, t^*)$ is the thickness of the water layer perpendicular to the bedrock, and N is the recharge rate.

[6] A generalized variant of equation (5) is due to *Rupp and Selker* [2006] who relaxed the assumption of uniform conductivity, instead allowing conductivity k to vary with depth as a power-law:

$$\frac{\partial h^*}{\partial t^*} = \frac{k_D}{fD^n(n+1)} \frac{\partial}{\partial x^*} \left[h^{*,n+1} \left(\frac{\partial h^*}{\partial x^*} \cos \alpha + \sin \alpha \right) \right] + \frac{N}{f} \quad (6)$$

where k_D is the saturated hydraulic conductivity at distance D perpendicular above the bedrock. The constant n is the exponent that describes the rate of change in saturated hydraulic conductivity k with distance perpendicular to the aquifer base. When $n = 0$ (i.e., vertical homogeneity in k), equation (6) reduces to equation (5).

[7] Application of the method of *Brutsaert and Nieber* [1977], i.e., linking recession parameters a and b to aquifer properties, to sloping aquifers requires analytical solutions to equation (5) or (6). *Daly and Porporato* [2004] have provided the only known exact solutions, which are for special cases of flow in a homogeneous aquifer that is infinite in both the up and downslope directions. For more practical cases in finite aquifers, analytical solutions have mainly been arrived at by making the kinematic-wave approximation [e.g., *Henderson and Wooding*, 1964; *Beven*, 1981;

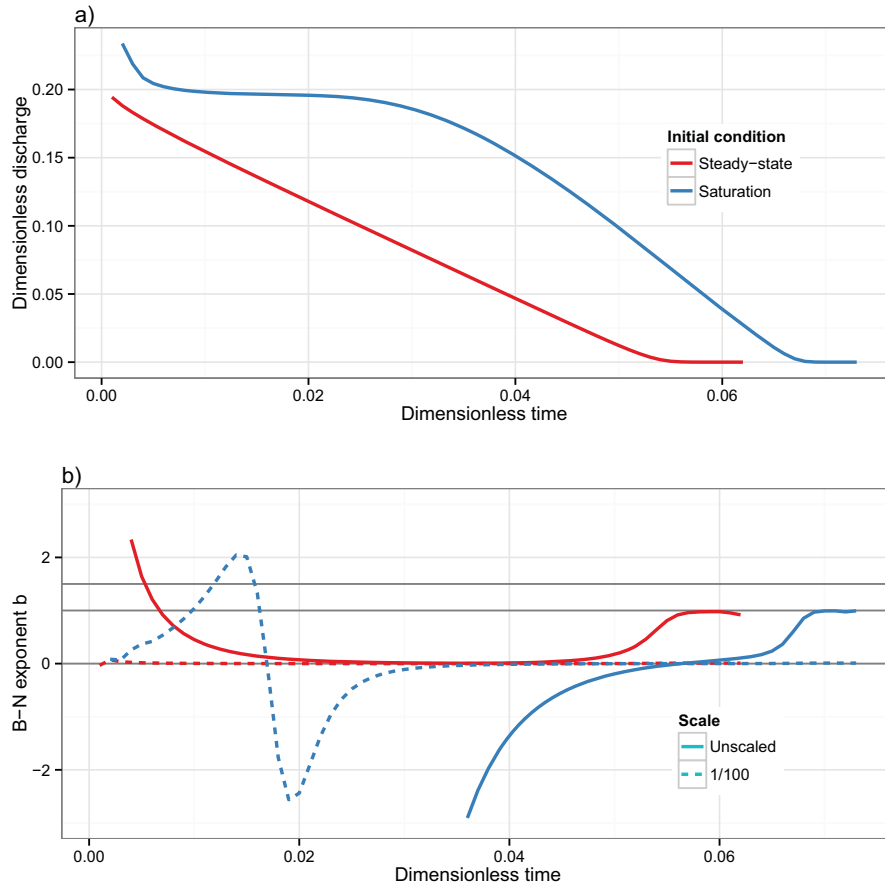


Figure 2. (a) Nondimensional hydrographs and (b) evolution of recession parameter b , for two types of initial conditions: Steady state and Saturation. $b/100$ is plotted in dashed lines to show the full range of b during recession.

Harman and Sivapalan, 2009a] or by linearizing the Boussinesq equation (see review in Rupp and Selker [2006]).

[8] Huyck *et al.* [2005] showed how an analytical solution to the linearized form of equation (5) leads to discharge of the form

$$-\frac{dQ}{dt} \approx aQ \quad (7)$$

after sufficient time has elapsed following the cessation of recharge to the aquifer, suggesting that $b \approx 1$. Brutsaert [1994, p. 2762], however, had warned of the (potential) lack of validity of the late-time result arising from the linearization of equation (5), when applied to steep shallow aquifers. This is because the linearized equation, unlike the nonlinear equation, does not permit the lowering water table, or drying front, to arrive at the impermeable base at the upslope aquifer boundary and then progress downslope along the aquifer base [Stagnitti *et al.*, 2004].

[9] Given the above limitations of linearization, Rupp and Selker [2006] made a closer examination of the late-time discharge behavior of equation (6) through numerical solutions of the nonlinear equation. They also arrived at the result given by equation (7) for $n = 0$, though their definition of the parameter a was different from Huyck *et al.*

[2005]. Furthermore, Rupp and Selker [2006] concluded that the late-time discharge could be approximated as

$$-\frac{dQ}{dt} \approx aQ^{\frac{2n+1}{n+1}} \quad (8)$$

for $n \geq 0$, which also suggest that $b = 1$ for the case of a homogeneous aquifer ($n = 0$). This result of $b = 1$ is in contradiction to the drainage behavior of steep hillslopes if one assumes that kinematic-wave assumptions holds. For steep hillslopes, the term $\partial h/\partial x$ in equation (3) becomes small with respect to $\sin \alpha$, such that $q \approx kh \sin \alpha$. It has been shown that under these circumstances (the discharge predicted by) the kinematic-wave equation is a good approximation of (the discharge predicted by) the Boussinesq equation [Henderson and Wooding, 1964; Beven, 1981].

[10] For constant k ($n = 0$), the kinematic recession behavior of such a hillslope will depend on initial conditions, where two extreme cases can be distinguished [Rupp and Selker, 2006]. First, prolonged rainfall on initial dry soil leads to the formation of a wedge-shaped steady state geometry of the saturated zone. For each location along the hillslope of length L , $q = N(L-x)$, such that $h = N(L-x)/(k \sin \alpha)$. During recession, this wedge travels downhill, with constant velocity such that $h(t)$ is linearly decreasing, and dQ/dt

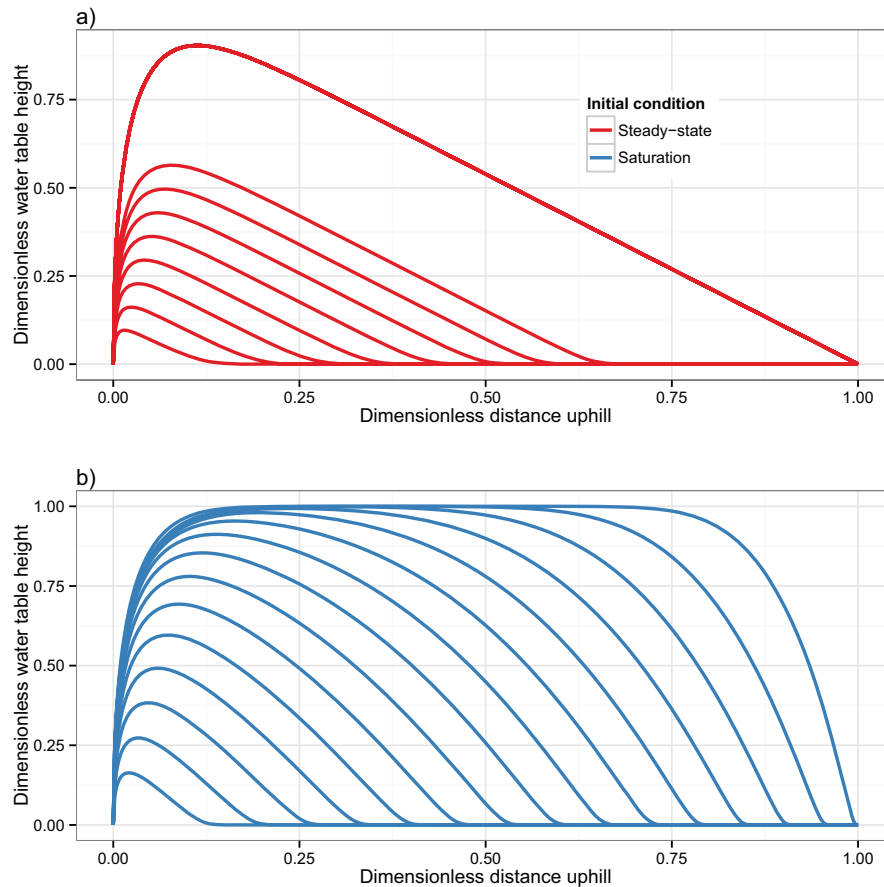


Figure 3. Nondimensional water tables during recession for two types of initial conditions: (a) Steady state and (b) Saturation.

a constant, such that $b = 0$. Second, after a short pulse-like rainstorm an initial dry soil becomes saturated to some depth h . During the poststorm recession period, this rectangular “saturated slab” travels downhill. Because h is constant, q is constant, and therefore $dQ/dt = 0$. Solving equation (1) for a and b yields $a = 0$ with b left undetermined. Note that *Rupp and Selker* [2006] in their Figure 3 mistakenly list $b = 0$ instead of $b = \text{undefined}$ for the uniform saturation case.

[11] A similar result (q decreasing linearly with time, the equivalent of $b = 0$) for the kinematic-wave approximation of the Boussinesq equation applied to the case of steep hillslopes with shallow soils was reached by [*Harman and Sivapalan*, 2009a], while investigating storage-discharge relationships derived from the Boussinesq equation for a range of forcing and boundary conditions. However, as shown above, the value of b that arises from the kinematic-wave approximation “long” after the cessation of recharge is dependent upon the profile of the water table at the onset of recession, which is in turn dependent on the history of recharge events. Whether the kinematic wave approximation is an accurate representation of the behavior of the nonlinear Boussinesq equation, in terms of dQ/dt versus Q , has not, to our knowledge, been demonstrated.

[12] The aim of this paper is to investigate the behavior of b in numerical solutions of the nonlinear Boussinesq equation, to evaluate to what extent the results of $b = 1$ in

the literature are due to the physics of the system (in case of b derived from observations), or caused by numerical artifacts (in case of b derived from numerical simulations). These results are relevant for any interpretation of field observed a and b for steep hillslopes and catchments, analogous to the application of equation (2a) to flat-lying aquifers. These results are also relevant for our understanding of the numerical aspects of hydrological models [*Kavetski et al.*, 2003; *Clark and Kavetski*, 2010; *Kavetski and Clark*, 2010].

2. Methods

[13] Several schemes to nondimensionalize equation (5) are proposed, which differ mainly in how the vertical dimension h is scaled. *Stagnitti et al.* [2004] scale h by an initial saturated thickness D . This approach is especially useful in combination with the linearized Boussinesq equation, because the linearization process involves replacing a dynamic water table height h with a constant water table height $\propto D$. For the nonlinear Boussinesq equation, this advantage does not hold, and might even turn into a disadvantage if a steady state initial condition is used, and D loses its original meaning.

[14] The nondimensionalization scheme proposed by *Harman and Sivapalan* [2009a] circumvents this problem

by scaling h by the hillslope height $L \tan \alpha$. Although this removes the need for a potentially arbitrarily chosen D , it prevents the application to flat aquifers, where $L \tan \alpha = 0$.

[15] Because we want to illustrate the solutions ranging from flat aquifers to steep slopes, we follow *Stagnitti et al.* [2004] and nondimensionalize equation (5) by defining the dimensionless distance x , dimensionless water table height h , and dimensionless time t , defined as

$$x = x^*/L, \quad h = h^*/D, \quad t = \frac{Dk \cos \alpha}{fL^2} t^* \quad (9)$$

[16] Combining equations (9) with (5) yields the nondimensional Boussinesq equation

$$\frac{\partial h}{\partial t} = \frac{\partial}{\partial x} \left(h \frac{\partial h}{\partial x} \right) + U \frac{\partial h}{\partial x} + S \quad (10)$$

where

$$U = \frac{L \tan \alpha}{D} \quad \text{and} \quad S = \frac{L^2 N}{D^2 k \cos \alpha} \quad (11)$$

[17] Equation (10) can be solved numerically by finite difference models in various ways. In order to ensure that our result does not depend on a given solution technique, multiple model variants were tested.

2.1. Diffusion Term

[18] We distinguish between two types of finite differencing of the diffusion term $\nabla(h\nabla h)$ in equation (10). In Type I the origin of this diffusion term, the gradient of the flux, ∇q , is preserved within the finite-differencing scheme:

$$\begin{aligned} & \frac{\partial}{\partial x} \left(h \frac{\partial h}{\partial x} \right) \\ & \approx \frac{1}{\Delta x} \left[\left(\frac{h_r + h_i}{2} \right) \left(\frac{h_r - h_i}{\Delta x} \right) - \left(\frac{h_i + h_l}{2} \right) \left(\frac{h_i - h_l}{\Delta x} \right) \right] \\ & \approx \frac{h_r^2 + h_i^2 - 2h_i^2}{2(\Delta x)^2} \end{aligned} \quad (12)$$

with $h_l = h_{i-1}^j$ (left, downwind), and $h_r = h_{i+1}^j$ (right, upwind). With i the spatial node and j the current temporal step. This approach is followed by, for example, *Stagnitti et al.* [2004]. Alternatively, in Type II the diffusion term is expanded completely by applying the product rule as

$$\begin{aligned} \frac{\partial}{\partial x} \left(h \frac{\partial h}{\partial x} \right) &= \left(\frac{\partial h}{\partial x} \right)^2 + h \frac{\partial^2 h}{\partial x^2} \\ &\approx \left(\frac{h_r - h_l}{2\Delta x} \right)^2 + h_i \left(\frac{h_r + h_l - 2h_i}{(\Delta x)^2} \right) \end{aligned} \quad (13)$$

[19] This approach was applied by *Troch et al.* [2003] while developing the *hillslope storage Boussinesq* model.

2.2. Spatial Derivatives

[20] Spatial derivatives such as $\partial h/\partial x$ can be discretized by using an upwind scheme (applied by, e.g., *Rupp and Selker* [2006]), a downwind scheme (apparently applied by

Stagnitti et al. [2004]), or a centered scheme (applied by, e.g., *Beven* [1981]; *Upadhyaya and Chauhan* [2001]). For advection-dominated problems, such as equation (5) applied to steep hillslopes, upwind schemes are used more often than centered or downwind schemes because of their greater stability [*Slingerland and Kump*, 2011]. For this reason downwind schemes were not used in this study, because they suffer the most from stability problems.

2.3. Temporal Derivatives

[21] A fully explicit Type I upwind scheme is derived as

$$H_i = h_i + \frac{\Delta t}{2(\Delta x)^2} [h_i^2 + h_r^2 - 2h_i^2] + \frac{U\Delta t}{\Delta x} (h_r - h_i) + N\Delta t \quad (14)$$

where $H_i = h_i^{j+1}$. Fully implicit or Crank-Nicolson schemes are obtained by rewriting equation (14) as a coupled set of equations

$$H_i = h_i + \frac{\Delta t}{2(\Delta x)^2} [H_i^2 + H_r^2 - 2H_i^2] + \frac{U\Delta t}{\Delta x} (H_r - H_i) + N\Delta t \quad (15)$$

and solving these simultaneously for all H_i . In order to solve the corresponding tridiagonal set of equations, the three quadratic H terms in equation (15) have to be linearized. We applied the suggestion by *Chapman* [2005] (their equation (14)) to use $H = h + \Delta h = h + (H - h)$ such that

$$\begin{aligned} H^2 &= h^2 + 2h(H - h) + (H - h)^2 \\ &\approx h^2 + 2h(H - h) \\ &\approx 2Hh - h^2 \end{aligned} \quad (16)$$

thus ignoring a (very small) $(\Delta h)^2$ term.

[22] Centered and Type II schemes are derived in a similar fashion.

2.4. Boundary Conditions

[23] We use a fixed boundary condition (B.C.) $h = 0$ at the foot of the hillslope ($x = 0$), and apply a no-flux condition at $x = L$. Finite differencing the Darcy equation (3) and solving for h_r results in $h_r = h_l - 2\Delta x(L/D)\tan \alpha$ for a centered scheme and $h_r = h_l - \Delta x(L/D)\tan \alpha$ for an upwind scheme.

[24] Associated with the upslope boundary is the development of a drying front, which can be explicitly tracked within the model [*Stagnitti et al.*, 2004]. Once a given $h_f \leq 0$, all $h_{i \geq f}$ are optionally fixed at $h = 0$.

2.5. Initial Conditions

[25] Two types of initial conditions (I.C.) were used: ‘‘Steady State’’ and ‘‘Saturation.’’ For the ‘‘Steady State’’ I.C., the model starts with an empty aquifer and is subjected to steady recharge N . Once steady state is effectively achieved ($\partial h/\partial t = 0$ and $q = N$) recharge is stopped and the subsequent recession hydrograph is recorded. For the ‘‘Saturation’’ I.C., $h = 1$ is set for all $x > 0$, after which recession starts.

3. Results

[26] Various combinations of above numerical schemes and conditions were run, using the following default

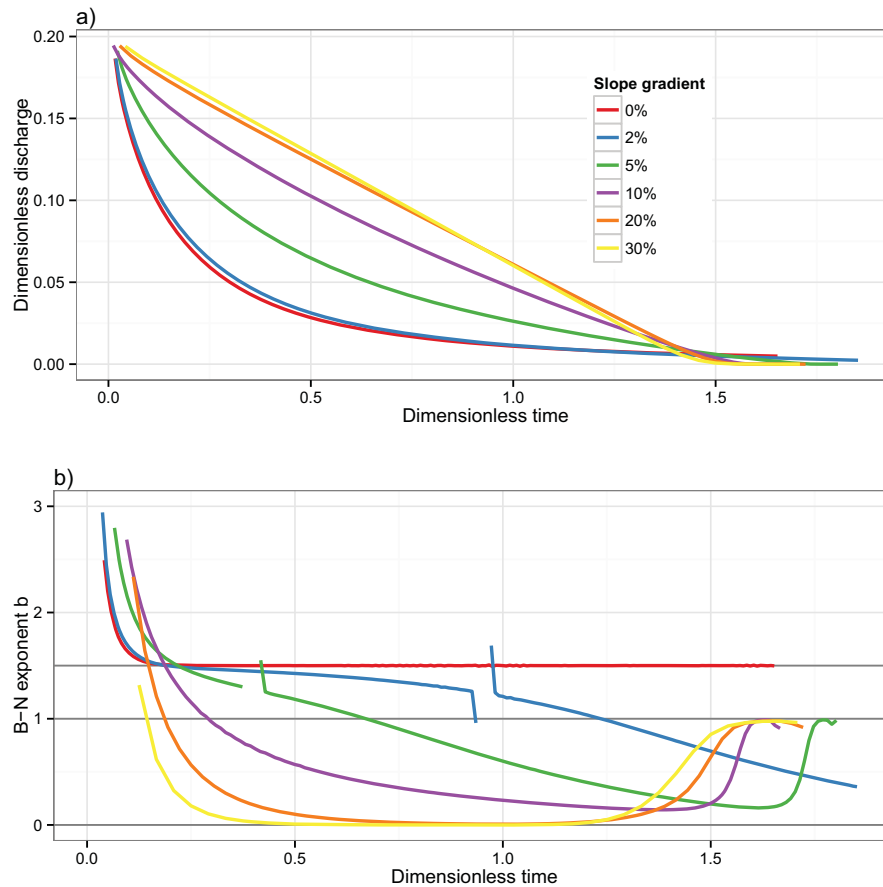


Figure 4. (a) Nondimensional hydrographs and (b) evolution of recession parameter b , for a range of slope gradient (0–30%), using a Steady state I.C.

parameters: $L = 100$ m; $\alpha = 20\%$; $D = 1$ m; $N = 10$ mm/d; and $k = 5$ m/d from which the dimensionless parameters $U = 20.0$ and $S = 20.4$ were computed. The model was run with automatic time step control, using the smaller of $\Delta t \leq \Delta x^2/2$ (stability criterion of the diffusion component) and $\Delta t \leq \Delta x/U$ (Courant stability criterion of the advection component) [Slingerland and Kump, 2011]. Time steps were decreased by an extra factor of 5 or higher to remove fluctuations and further constrain truncation errors. Recession discharge Q was computed from bookkeeping the water balance, because direct application of equation (3) is not possible due to the $h = 0$ B.C. Instead of fitting the power-law equation (1) to the whole Q , $-dQ/dt$ output data cloud, we applied a more dynamic approach and computed a and b for every three successive Q , $-dQ/dt$ output data points, resulting in the temporal evolution of a and b during the recession. Note that since evaporation and instream flows are not included in our model, the suggestion by Brutsaert and Nieber [1977] to use the lower envelope of the Q , $-dQ/dt$ data to correct for evaporation effects (resulting in higher $-dQ/dt$ during recession), does not apply.

[27] The results of various spatial difference schemes (upwind versus centered, Type I versus Type II), in combination with optional explicit tracking of the drying front, are shown in Figure 1. It can be seen that the recession hydrograph is very slightly concave to linear, until it appa-

rently empties. Note that just before $Q = 0$ the hydrographs makes a gentle bend, i.e., the transition from “drainage” to “empty” is not sharp. This general behavior is reflected in the evolution of recession parameter b from equation (1). It is clearly visible that during early recession b starts at high values (cut off at $b = 3$ in Figures 1b, 2b, etc.) after which b asymptotically approaches $b = 0$. Around the time the aquifer is nearly emptied, and q approaches 0, b rises to $b = 1$. Based on this general behavior, we distinguish periods: early recession ($0 < t < 0.01$), late recession ($0.01 < t < 0.05$), and postrecession ($t > 0.05$). Note that the timing is dependent on advection parameter U . This behavior is consistent for all model variants plotted. Note that the centered Type II variants display slightly unstable b -behavior (both for Runge-Kutta and for Crank-Nicolson numerical methods) although the general pattern is still consistent with the other variants, except for the postrecession values of $b \approx 1.5$ (again, both for Runge-Kutta and for Crank-Nicolson numerical methods).

[28] Because of the similar results for centered and upwind schemes, the general preference for upwind schemes for advection-dominated problems [Slingerland and Kump, 2011], and the higher stability of the Type I scheme, subsequent simulations are carried out with the upwind Type I scheme without tracking of the drainage front.

[29] Fully explicit, fully implicit, and Crank-Nicolson schemes all gave identical results (not shown).

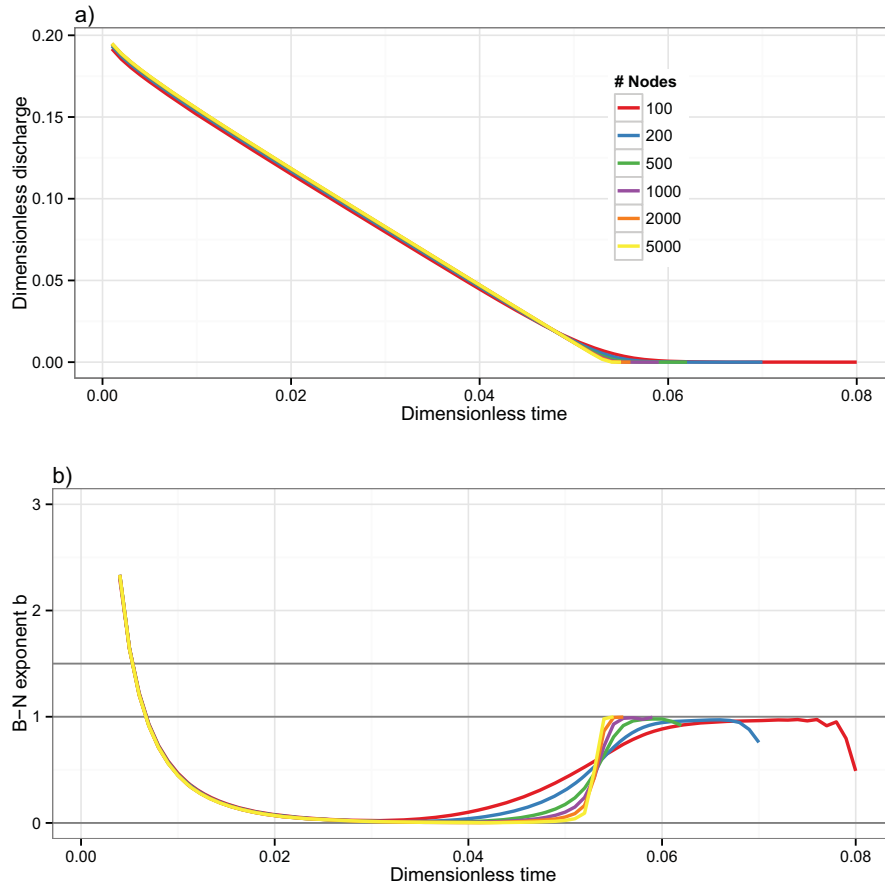


Figure 5. (a) Nondimensional hydrographs and (b) evolution of recession parameter b for a range of number of nodes (100–2000), using a Steady state I.C.

[30] Figure 2 shows the results for a comparison between Steady State and Saturation initial conditions. The recession resulting from initial saturation is more complex, with b first (highly) positive, then (highly) negative after which the behavior becomes similar to that of the Steady State I.C. recession: a period where $b \approx 0$ to finally a period where $b \approx 1$ (postrecession).

[31] The behavior of b can be understood if one considers the hydrograph, and the reasoning put forward in the discussion of kinematic-wave hillslopes in the Introduction section. For clarity, water tables for this simulation are shown in Figure 3. It can be clearly seen that for the Steady State I.C., the saturated zone takes the general shape of a wedge (except for the curvature toward $h = 0$ at $x = 0$ due to the B.C.) that slides down the hillslope creating $b \approx 0$. The Saturation I.C. starts off with some rapid drainage of the near-surface areas near $x = 0$ and $x = 1$ after which a (rounded) rectangular slab remains that first slides downhill (resulting in approximately constant q and b fluctuating around zero) which slowly transforms into a wedge similar as in the Steady State I.C. case (resulting in similar b evolution from this point onward).

[32] Figure 4 shows the response of the Boussinesq equation for a range of slope gradients and the Steady State I.C. It can be clearly seen that the evolution of b for steep hillslopes (20–30%) is completely different than that for

flat-lying aquifers. For the latter, we find the classical value of $b = 3/2$ [Brutsaert and Nieber, 1977]. The steeper the hillslope, the more b approaches 0. This is consistent with the notion that for steep hillslopes the kinematic terms dominate, such that the kinematic-wave assumptions increasingly are being met, which predict $b = 0$ (as outlined in the Introduction).

[33] The steepness of the transition from the late-recession $b \approx 0$ to the postrecession $b \geq 1$ regime depends on the number of nodes used in the finite-differencing scheme. In Figure 5, the results are shown for number of nodes ranging from 100 to 5000 nodes. The more nodes, the steeper the transition. We interpret these results as indicating the inability of numerical approximations of the Boussinesq equation to make a sharp transition from “slightly wet” to “completely dry.” Extrapolating these results it may be surmised that an infinite number of nodes would lead to either an instantaneous transition from $b = 0$ to $b \geq 1$, or termination of discharge from the model because the storage is expended. Physical realism dictates that termination of discharge would be the correct extrapolation.

[34] Figure 6 shows that the $b = 0$ behavior of the model during normal recession is insensitive for variant parameter settings. Parameters L and D directly affect the nondimensional advection term U of equation (10), which varies over

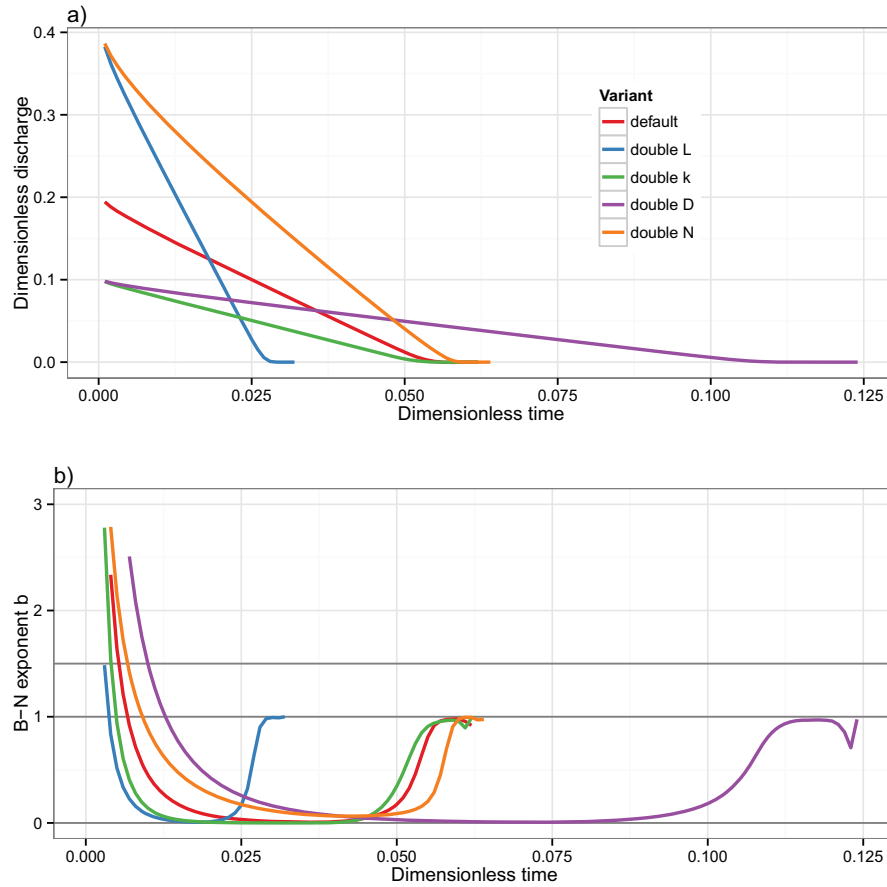


Figure 6. (a) Nondimensional hydrographs and (b) evolution of recession parameter b for doubled (with respect to the default run) values of parameters L , k , D , and N , using a Steady state I.C.

a range 10–40, and cause a response in hydrograph timing, while L , k , D , and N affect source term S and cause a response in initial steady state discharge, as expected.

4. Discussion and Conclusions

[35] It is shown that for the Boussinesq equation applied to steep aquifers with constant k , the recession behavior is dominated by values of b approaching $b = 0$. This result is robust with respect to variety of numerical schemes. The “late time recession” $b = 1$ reported earlier [Rupp and Selker, 2006] has to be considered an artifact of the inability of numerical approximations to make the transition from drainage to complete dryness. In the model output, this transition is visible as a gentle bend in $Q(t)$ diagrams when Q approaches $Q = 0$. Similar bends are visible in hydrographs computed with numerical implementations of the Boussinesq equation as reported in the literature, e.g., see [Harman and Sivapalan, 2009a, Figure 2b] or [Basha and Maalouf, 2005, Figure 3]. Because $Q = 0$ is only asymptotically reached, this bend, while small in terms of Δt , becomes large in terms of $\Delta \log Q$ when plotted in the $\log -dQ/dt$ versus $\log Q$ diagram traditionally used to infer a and b , thus could easily give rise to the misinterpretation of $b = 1$ (though Harman and Sivapalan [2009a] and Basha and Maalouf [2005] make no mention of this artifact and it apparently was not a factor in their analyses).

[36] It is suggested that this postrecession $b \geq 1$ does not have physical meaning in a sloping aquifer, both because it is not supported by groundwater flow theory as represented by the Boussinesq equation, and because this change from $b = 0$ to $b = 1$ due to saturated flow will not occur in actual porous media. When natural aquifers are subjected to extensive drainage to the point that saturated zones disappear totally, other (capillary) forces that are not included in the assumptions underlying the Boussinesq equation will dominate the hydrological processes.

[37] It is of interest to compare our observations with the exact analytical solution of Daly and Porporato [2004] for a spreading mound of water initially concentrated at a point $x = x_0$ in an infinite aquifer. Considering the time following passage of the mound’s peak at a point x downslope from x_0 , it can be shown that the influence of the initial conditions wanes over time and the time rate of change in discharge at x approaches a constant value that is solely a function of the static aquifer properties:

$$-\frac{dQ}{dt} \approx \frac{k^2}{9f} \tan \alpha \sin^2 \alpha \quad (17)$$

which is to say that b approaches a value of 0. Thus, at least free from any influencing up- or downslope boundary condition, the nonlinear Boussinesq equation does not generate an exponentially decreasing late-time recession curve where slope is a significant factor.

[38] The value of $b \approx 0$ found here is consistent with multiple lines of evidence: the numerical results shown here, the analogy with a kinematic-wave wedge sliding down a hillslope, and the analytical results for infinite-length hillslopes *Daly and Porporato* [2004].

[39] One possible explanation why numerical approximations to the nonlinear Boussinesq equation display $b = 1$ during postrecession is due to properties of hydrographs than can be derived from the power-law equation (1). Writing this as

$$-\frac{1}{aQ^b}dQ = dt \quad (18)$$

and integrating

$$-\frac{1}{a} \int Q^{-b} dQ = \int dt \quad (19)$$

one yields

$$Q(t) = \begin{cases} c_1 e^{-at} & \text{for } b=1 \\ \frac{1}{[(b-1)(at+c_2)]^{1-b}} & \text{for } b \neq 1 \end{cases} \quad (20)$$

with c_1 and c_2 appropriate constants of integration. The total volume water draining from a hillslope aquifer, V is obtained by further integration of equation (20). Three cases can be distinguished: For $b < 1$, equation (20) only has real solutions for $t \leq -c_2/a$. When $t = -c_2/a$, $Q = 0$, and the entire reservoir is empty, after draining a finite volume $V = \int_0^{-c_2/a} Q(t) dt$. For $1 \leq b < 2$, the integral $V = \int_0^\infty Q(t) dt$ exists, meaning that a finite volume of water V drains from a catchment during an infinite recession. For $b \geq 2$ this integral has an infinite solution which implies that an infinite volume of water drains from this hillslope during an infinite recession (cf. TOPMODEL [*Beven and Kirkby*, 1979], where the exponential k -profile results in $b = 2$ and infinite storage, which is solved by using storage deficit rather than storage as state variable). This implies that numerical models that are unable to drain completely (i.e., in finite time) are not consistent with $b < 1$ behavior, suggesting that such models by necessity must adopt $b \geq 1$ behavior eventually, which is exactly what we see in all our model implementations.

[40] The implication of these results is that the nonlinear Boussinesq equation in combination with the assumption of constant k is not able to represent late-time behavior for many steeply sloping experimental watersheds and field studies, where b is commonly found to be in the range 1–2 [*Wittenberg*, 1999; *Lyon and Troch*, 2007; *Kirchner*, 2009]. This implies that when inferring catchment-scale aquifer properties using the *Brutsaert and Nieber* [1977] method, geometric similarity of a representative, unit-width, homogeneous, and sloping Boussinesq aquifer is an improper assumption; real catchments will be composed of numerous hillslopes and valley bottoms of varying shapes, sizes, soils, and aquifer materials. It is likely that the observed values of b reflect vadose zone influences [*Chapman*, 2003; *Szilagyi*, 2004; *Rupp et al.*, 2009], evapotranspiration [*Brutsaert*, 1982], complex aquifer geometry

[*Troch et al.*, 2003], active stream network morphology [*Biswal and Marani*, 2010], and spatial heterogeneity in catchment properties [*Harman and Sivapalan*, 2009b; *Harman et al.*, 2009]. In particular, heterogeneity would cause some water to be retained longer in the catchment.

[41] One other implication is that the exponential decline ($b = 1$) in late time resulting from the commonly used linearized form of the Boussinesq equation is also an artifact, although a product of linearization, because this prevents the formation of a drying front [*Stagnitti et al.*, 2004]. The absence of a drying front leads to infinite recession and thus $b \geq 1$, as demonstrated above. One consequence is that the use of this linearized solution at late time to accurately infer hydraulic properties of sloping aquifers from observations of streamflow becomes more problematic. This is because the linearized Boussinesq equation is not able to adequately approximate the recession behavior, in terms of b , as simulated by the nonlinear Boussinesq equation, which is the reference for the linearized equation. This conclusion is independent of the fact that values for $b = 1$ as derived from streamflow observations is consistent with $b = 1$ resulting from the linearized Boussinesq equation.

[42] It is suggested that future applications of the Boussinesq equation to real-world data consider alternative assumptions regarding hydraulic architecture, such as those that lead to a decrease in aquifer conductivity with decreasing storage, e.g., the exponential decreasing k profile of TOPMODEL [*Beven and Kirkby*, 1979] (but see *Kavetski et al.* [2003] and *Clark and Kavetski* [2010] for numerical issues here), resulting in $b = 2$ or the power-law k profiles of *Rupp and Selker* [2006], resulting in $1 < b < 2$. This would be a worthwhile effort, because verification of the numerical solution to equation (6) for $n > 0$, suggest that, if the recession signal is not dominated by above mentioned factors, equation (1) could be used to infer hydraulic properties of aquifers that have power-law-like saturated hydraulic conductivity profiles, enabling the use of large-scale conceptual models that do have physical meaning. Careful consideration, however, still needs to be made of the scale at which equation (1) is applied, as equation (6) is strictly for a single hillslope.

[43] Finally, we stress that these results do not invalidate the general utility of the sloping Boussinesq equation, but rather some of the assumptions used in applications.

[44] **Acknowledgments.** This research was partly funded by NWO (Netherlands Organization for Scientific Research) project 857.00.008, and the Oregon Experiment station. The authors thank P. Torfs for pointing out the different finite-differencing options, D. Kavetski for useful suggestions, and three anonymous reviewers for their thoughtful comments that helped improving the manuscript.

References

- Basha, H. A., and S. F. Maalouf (2005), Theoretical and conceptual models of subsurface hillslope flows, *Water Resour. Res.*, *41*, W07018, doi: 10.1029/2004WR003769.
- Beven, K. (1981), Kinematic subsurface stormflow, *Water Resour. Res.*, *17*, 1419–1424, doi:10.1029/WR017i005p01419.
- Beven, K. J., and M. J. Kirkby (1979), A physically based, variable contributing area model of basin hydrology, *Hydrol. Sci. J.*, *24*(1), 43–69, doi: 10.1080/02626667909491834.
- Biswal, B., and M. Marani (2010), Geomorphological origin of recession curves, *Geophys. Res. Lett.*, *37*, L24403, doi:10.1029/2010GL045415.

- Brutsaert, W. (1982), *Evaporation Into the Atmosphere: Theory, History, and Applications*, Kluwer Acad., Dordrecht, doi:10.1007/978-94-017-1497-6.
- Brutsaert, W. (1994), The unit response of groundwater outflow from a hillslope, *Water Resour. Res.*, *30*, 2759–2763, doi:10.1029/94WR01396.
- Brutsaert, W., and J. P. Lopez (1998), Basin-scale geohydrologic drought flow features of riparian aquifers in the southern Great Plains, *Water Resour. Res.*, *34*, 233–240, doi:10.1029/97WR03068.
- Brutsaert, W., and J. L. Nieber (1977), Regionalized drought flow hydrographs from a mature glaciated plateau, *Water Resour. Res.*, *13*, 637–643, doi:10.1029/WR013i003p00637.
- Chapman, T. G. (2003), Modelling stream recession flows, *Environ. Modell. Software*, *18*, 683–692, doi:10.1016/S1364-8152(03)00070-7.
- Chapman, T. G. (2005), Recharge-induced groundwater flow over a plane sloping bed: Solutions for steady and transient flow using physical and numerical models, *Water Resour. Res.*, *41*, W07027, doi:10.1029/2004WR0036.
- Clark, M. P., and D. Kavetski (2010), Ancient numerical daemons of conceptual hydrological modeling: 1. Fidelity and efficiency of time stepping schemes, *Water Resour. Res.*, *46*, W10510, doi:10.1029/2009WR008894.
- Daly, E., and A. Porporato (2004), A note on groundwater flow along a hillslope, *Water Resour. Res.*, *40*, W01601, doi:10.1029/2003WR002438.
- Eng, K., and W. Brutsaert (1999), Generality of drought flow characteristics within the Arkansas River basin, *J. Geophys. Res.*, *104*, 19,435–19,441, doi:10.1029/1999JD900087.
- Harman, C., and M. Sivapalan (2009a), A similarity framework to assess controls on shallow subsurface flow dynamics in hillslopes, *Water Resour. Res.*, *45*, W01417, doi:10.1029/2008WR007067.
- Harman, C., and M. Sivapalan (2009b), Effects of hydraulic conductivity variability on hillslope-scale shallow subsurface flow response and storage-discharge relations, *Water Resour. Res.*, *45*, W01421, doi:10.1029/2008WR007228.
- Harman, C. J., M. Sivapalan, and P. Kumar (2009), Power law catchment-scale recessions arising from heterogeneous linear small-scale dynamics, *Water Resour. Res.*, *45*, W09404, doi:10.1029/2008WR007392.
- Henderson, F. M., and R. A. Wooding (1964), Overland flow and groundwater flow from a steady rainfall of finite duration, *J. Geophys. Res.*, *69*, 1531–1540, doi:10.1029/JZ069i008p01531.
- Huyck, A. A. O., V. R. N. Pauwels, and N. E. C. Verhoest (2005), A base flow separation algorithm based on the linearized Boussinesq equation for complex hillslopes, *Water Resour. Res.*, *41*, W08415, doi:10.1029/2004WR003789.
- Kavetski, D., and M. P. Clark (2010), Ancient numerical daemons of conceptual hydrological modeling: 2. Impact of time stepping schemes on model analysis and prediction, *Water Resour. Res.*, *46*, W10511, doi:10.1029/2009WR008896.
- Kavetski, D., G. Kuczera, and S. W. Franks (2003), Semidistributed hydrological modeling: A “saturation path” perspective on TOPMODEL and VIC, *Water Resour. Res.*, *39*(9), 1246, doi:10.1029/2003WR002122.
- Kirchner, J. W. (2009), Catchments as simple dynamical systems: Catchment characterization, rainfall-runoff modeling, and doing hydrology backward, *Water Resour. Res.*, *45*, W02429, doi:10.1029/2008WR006912.
- Lyon, S. W., and P. A. Troch (2007), Hillslope subsurface flow similarity: Real-world tests of the hillslope Péclet number, *Water Resour. Res.*, *43*, W07450, doi:10.1029/2006WR005323.
- Pauwels, V. R. N., and P. A. Troch (2010), Estimation of aquifer lower layer hydraulic conductivity values through base flow hydrograph rising limb analysis, *Water Resour. Res.*, *46*, W03501, doi:10.1029/2009WR008255.
- Rupp, D. E., and J. S. Selker (2006), On the use of the Boussinesq equation for interpreting recession hydrographs from sloping aquifers, *Water Resour. Res.*, *42*, W12421, doi:10.1029/2006WR005080.
- Rupp, D. E., J. Schmidt, R. A. Woods, and V. Bidwell (2009), Analytical assessment and parameter estimation of a low-dimensional groundwater model, *J. Hydrol.*, *377*, 143–154, doi:10.1016/j.jhydrol.2009.08.018.
- Slingerland, R., and L. Kump (2011), *Mathematical Modeling of Earth's Dynamical Systems; A Primer*, 231 pp., Princeton Univ. Press, Princeton.
- Stagnitti, F., L. Li, J.-Y. Parlange, W. Brutsaert, D. A. Lockington, T. S. Steenhuis, M. B. Parlange, D. A. Barry, and W. L. Hogarth (2004), Drying front in a sloping aquifer: Nonlinear effects, *Water Resour. Res.*, *40*, W04601, doi:10.1029/2003WR002255.
- Szilagyi, J. (2004), Vadose zone influences on aquifer parameter estimates of saturated-zone hydraulic theory, *J. Hydrol.*, *286*, 78–86, doi:10.1016/j.jhydrol.2003.09.009.
- Szilagyi, J., M. B. Parlange, and J. D. Albertson (1998), Recession flow analysis for aquifer parameter determination, *Water Resour. Res.*, *34*, 1851–1857, doi:10.1029/98WR01009.
- Troch, P. A., F. P. De Troch, and W. Brutsaert (1993), Effective water table depth to describe initial conditions prior to storm rainfall in humid regions, *Water Resour. Res.*, *29*(2), 427–434, doi:10.1029/92WR02087.
- Troch, P. A., C. Paniconi, and E. Emiel van Loon (2003), Hillslope-storage Boussinesq model for subsurface flow and variable source areas along complex hillslopes: 1. Formulation and characteristic response, *Water Resour. Res.*, *39*(11), 1316, doi:10.1029/2002WR001728.
- Upadhyaya, A., and H. S. Chauhan (2001), Falling water tables in horizontal/sloping aquifer, *J. Irrig. Drain. Eng.*, *127*, 378–384, doi:10.1061/(ASCE)0733-9437(2001)127:6(378).
- van de Giesen, N., T. S. Steenhuis, and J.-Y. Parlange (2005), Short- and long-time behavior of aquifer drainage after slow and sudden recharge according to the linearized Laplace equation, *Adv. Water Resour.*, *28*, 1122–1132, doi:10.1016/j.advwatres.2004.12.002.
- Wittenberg, H. (1999), Baseflow recession and recharge as nonlinear storage processes, *Hydrol. Processes*, *13*, 715–726.